

Accepted Manuscript

The effect of hydroxylated fatty acid-containing phospholipids in the remodeling of lipid membranes

Stefano Piotto, Alfonso Trapani, Erminia Bianchino, Maitane Ibarguren, David J. López, Simona Concilio



DOI: doi: [10.1016/j.bbamem.2014.01.014](https://doi.org/10.1016/j.bbamem.2014.01.014)

To appear in: *BBA - Biomembranes*

Received date: 30 September 2013

Received in revised form: 11 January 2014

Accepted date: 13 January 2014

Please cite this article as: Stefano Piotto, Alfonso Trapani, Erminia Bianchino, Maitane Ibarguren, David J. López, Simona Concilio. The effect of hydroxylated fatty acid-containing phospholipids in the remodeling of lipid membranes. *BBA - Biomembranes* (2014), doi: [10.1016/j.bbamem.2014.01.014](https://doi.org/10.1016/j.bbamem.2014.01.014)

This is a PDF file of an unedited manuscript that has been accepted for publication. As a service to our customers we are providing this early version of the manuscript. The manuscript will undergo copyediting, typesetting, and review of the resulting proof before it is published in its final form. Please note that during the production process errors may be discovered which could affect the content, and all legal disclaimers that apply to the journal pertain.

## The effect of hydroxylated fatty acid-containing phospholipids in the remodeling of lipid membranes

Stefano Piotto<sup>1,\*</sup>, Alfonso Trapani<sup>1</sup>, Erminia Bianchino<sup>1</sup>, Maitane Ibarguren<sup>2</sup>, David J. López<sup>2</sup>, Simona Concilio<sup>3</sup>

<sup>1</sup> Department of Pharmacy, University of Salerno, via Giovanni Paolo II, 132 Fisciano 84084 SA – Italy

<sup>2</sup> Laboratory of Molecular Cell Biomedicine, University of the Balearic Islands-Lipopharma Therapeutics, S.L., Palma, Spain

<sup>3</sup> Department of Industrial Engineering, University of Salerno, via Giovanni Paolo II, 132 Fisciano 84084 SA – Italy

\*To whom correspondence should be addressed:

Stefano Piotto. Department of Pharmacy, University of Salerno, via Giovanni Paolo II, 132 Fisciano 84084 SA – Italy. Tel.: +39 320 4230068 ; Fax +39 089 969602; E-mail:

[piotto@unisa.it](mailto:piotto@unisa.it)

### Abstract

The synthetic fatty acid 2-hydroxyoleic acid (2OHOA) is an antitumor drug that regulates membrane lipid composition and structure. An important effect of this drug is the restoration of sphingomyelin (SM) levels in cancer cell membranes, where the SM concentration is lower than in non-tumor cells. It is well known that free fatty acids concentration in cell membranes is lower than 5%, and that fatty acid excess is rapidly incorporated into phospholipids. In a recent work, we have considered the effect of free 2OHOA in model membranes in liquid ordered (Lo) and liquid disordered (Ld) phases, by using all-atom molecular dynamics. This study concerns membranes that are modified upon incorporation of 2OHOA into different phospholipids. 2OHOA-containing phospholipids have a permanent effect on lipid membranes, making Ld membrane surface more compact and less hydrated, whereas the opposite effect is observed in Lo domains. Moreover, the hydroxyl group of fatty acid chains increases the propensity of Ld model membranes to form hexagonal or other non-lamellar structures.

### Keywords

Lipid membrane, membrane physical state, 2OHOA, molecular dynamics

## 1. Introduction

Cells membranes are mainly composed of lipids and proteins. Their thickness of a few nanometers is sufficient to compartmentalize specific cell functions into organelles, and to separate the cytoplasm from the extracellular surroundings. Besides being a physical barrier, cell membranes participate in cell processes that lead to cell survival, differentiation, cell cycle arrest and cell death, among others. Lipids are by far the most chemically diverse class of biomolecules, with an average range of 1300–1500 different species in eukaryotes. The most abundant lipids in membranes are glycerolipids, such as phosphatidylcholine, phosphatidylethanolamine, phosphatidylserine, phosphatidylinositol or phosphatidic acid. They are amphipathic molecules with a hydrophobic region formed by diacylglycerol, which contains two fatty acid (FA) chains, varying in length and degree of unsaturation, esterified to glycerol. Sphingolipids, another major type of lipids in membranes, are also amphipathic molecules with a lipophilic part formed by a sphingosine base attached to one fatty acid residue. The large majority of FAs in the cell membranes are part of more complex lipid molecules such as glycerolipids, sphingolipids and sterol esters, or even acyl moieties in membrane proteins. However, 1–2% of the total membrane lipids are present as free fatty acids (FFA) [1].

FFAs are known to modify the structure of lipid membranes, subsequently affecting the activity of membrane proteins and downstream cell signaling processes. A study performed on the capping of immunoglobulins in lymphocytes showed that trans-unsaturated and saturated FFAs localize preferentially into gel phases, while cis-unsaturated FFAs partition preferentially into fluid phases and inhibit capping immunoglobulin [2]. Moreover, cis-unsaturated FFAs also produce alterations in the patterns of cytoskeleton and contractile proteins in lymphocytes; however, neither trans-unsaturated nor saturated FFAs show any effect [3]. Natural, non-hydroxylated FA and synthetic, 2-hydroxylated FA derivatives can induce reorganization of lipid microdomains in model membranes [4]. The addition of both natural and hydroxylated cisunsaturated FFAs to lipid vesicles causes a rapid incorporation of the FFAs into the lipid bilayers and an increase in membrane fluidity. Besides, those FFAs augment the proportion of liquid-disordered (Ld) structures and disrupt the liquid-ordered (Lo, lipid raft-like) domains, decreasing their size and enriching them in the Lo-prone lipids sphingomyelin (SM) and cholesterol (CHOL). This correlates with the observation that one of those 2-hydroxylated fatty acids, 2-hydroxyoleic acid (2OHOA) decreases the global order of the membrane and increases the packing of ordered domains [5].

## 2. Material and methods

### 2.1. Construction of computational molecular models of lipid membranes

In all cases, symmetric lipid bilayers were supplemented with water molecules and Na<sup>+</sup> and Cl<sup>-</sup> counter ions in order to obtain a density of ~0.997 g/ml. All membranes containing a hydroxylated phospholipid were formed using the R-(+)-2-OHOA enantiomer. Thus, membranes that incorporated the 2OHOA as part of the SM, POPC and POPE structure were obtained replacing a hydrogen atom of the C $\alpha$  of the oleic chain of SM, POPC and POPE molecules, respectively, with a hydroxyl group. The lipid composition and physical parameters of the Lo, Ld and Lo/Ld model membranes used are shown in Table 1.

### 2.2. Molecular dynamics simulation

All simulations were performed with the program YASARA [18] under NPT ensemble at 310 K and 1 atm by coupling the system with a Berendsen thermostat [19] and by controlling the pressure in the barostat pressure control mode implemented in this software. The potential energy per lipid molecule was calculated using the force field AMBER03 [20]. The geometry of the molecules was optimized by a semi-empirical AM1 method using the COSMO solvation model [21]. Partial atomic charges were calculated using the same level used in the Mulliken point charge approach [22]. Electrostatic interactions were calculated with a cutoff of 10.48 Å, and the long-range electrostatic interactions were handled by the Particle Mesh Ewald (PME) algorithm [23] using a sixth-order B-spline interpolation and a grid spacing of 1 Å. The leap-frog algorithm was used in all simulations with a 1.25 fs time step for intramolecular forces, 2.5 fs time step for intermolecular forces and the equilibration period was of 2 ns. The lipid bilayers were assembled and relaxed reducing the box dimension until the Van der Waals energy of the system started to increase [24,25] and the structural parameters of the membranes were comparable with experimental data [26]. To remove bumps and correct the covalent geometry, all the systems were energy-minimized. After removal of conformational stress by a short steepest descent minimization, the procedure continued by simulated annealing (time step 2 fs, atom velocities scaled

down by 0.9 every 10 steps) until convergence was reached, i.e. the energy improved by less than 0.05 kJ/mol per atom during 200 steps. A full description of the protocol is given in [24].

### 2.3. Theory/calculation

#### 2.3.1. Energies and structural parameters

Energies and structural parameters were calculated following standard procedures and equations [27]. The stability in model membranes was followed monitoring the potential energy per lipid unit. The energies are expressed in kcal/mol and were calculated using the force field AMBER03. The potential energy per lipid was calculated dividing the total potential energy of the membrane by the number of lipids. The thickness was determined as the average distance between the planes fitting the phosphorous atoms of the two layers. The polarization of water dipoles on the bilayer surface (expressed in Debye) was calculated averaging the dipole moment of water molecules with a distance of 4 Å from the membranes. For comparison, the dipole moment of a water molecule with AMBER03 charges and distances is around 2.35 D and the total dipole moment of water bulk is less than 0.037 D per molecule (dipole moment of the bulk divided by the number of water molecules). The error is calculated averaging 5 snapshots of the last 5 ns of simulations. The calculation of membrane properties as a function of the depth in the bilayer was performed dividing the membrane into rectangular slabs with 1 Å of thickness and perpendicular to the z axis (normal to the bilayer). This procedure was adopted to calculate the profiles of mass density and lateral pressure profile, as a function of z.

#### 2.3.2. Mass density profiles

The cross-sectional mass distribution analysis of the lipid bilayer provides valuable information about the structural changes in membranes. For lipids, the mass density profile indicates the atom distribution along the bilayer. These profiles are determined by dividing the simulation box along the normal direction to the bilayer into a number of thin slices of equal thickness and by finding the mass density of the atoms located in each slice followed by time averaging over a large number of snapshots evenly distributed over the simulation time interval (i.e., the last 25 ns of the 50 ns simulation). This approach can be used because the membranes remain approximately flat during all of the simulation period.

#### 2.3.3. Lateral pressure profile

The mechanical properties of a membrane can be described by all the forces acting in the plane of the bilayer. At equilibrium, the bilayer adjusts the area per lipid so that the sum of these forces or lateral pressures is zero. However, they may vary as a function of depth in the bilayer as expressed by the lateral pressure or stress profile across the bilayer,  $p(z)$ . Changes in the membrane lipid composition modify the shape of the lateral pressure profile, which then alters the amount of mechanical work associated with conformational changes in membrane proteins [28]. Comparison of the pressure profile of model membranes with those of FA-modified membranes by molecular dynamics is a valuable data because it cannot be experimentally measured [29]. The calculation of the lateral pressure profile was performed using the method described by Hardy [30], calculating the stress of membrane slices perpendicular to the z axis.

#### 2.3.4. Radial distribution function

The radial distribution function (RDF)  $g(r)$  describes numerical density of atoms as a function of distance from a reference atom. The RDF of atoms  $i$  relative to each other (i.e. N – N RDF) is given by:

$$RDF_i = \frac{1}{N_i} \left\langle \frac{n(r)}{4\pi r^2 dr} \right\rangle,$$

where  $N_i$  is the number of atoms  $i$  in the system,  $n(r)$  is the number of atoms in the spherical shell of radius  $r$  and thickness  $dr$  around the given atom, and  $4\pi r^2 dr$  is the ring volume;  $\langle \rangle$  denotes the time and ensemble average.

## 3. Results

### 3.1. Effect of incorporation of 2OHOA in *Lo* domains

The calculation of the potential energy per lipid molecule allowed a stability analysis of the lipids in the membrane environment. Physical and structural properties of bilayers were calculated following standard

procedures and formulae [27]. Table S1 showed the energy per lipid (Kcal/mol), the thickness of the membranes (Å), and the polarization of the water molecules (Debye, D) closer than 4 Å to the membrane surface. Fig. 1A showed a continuous decrease of the energy per lipid in lipid raft-like membranes, which correlated with a decrease in CHOL and a subsequent increase in SM content. The incorporation of 2OHOA in SM molecules increased the previously mentioned effect, possibly due to additional hydrogen bond formation between the lipids and water molecules. The observed decrease of potential energy per lipid was translated into higher lipid mobility and stability, which reached the minimum at ~30 mol% CHOL (SM:CHOL; 7:3 or SM:SMh:CHOL; 3.5:3.5:3; mol ratio).

Moreover, along with CHOL reduction, the raft-like domains became thicker. According to the umbrella model, CHOL molecules are normally covered by the SM headgroups, while SM molecules remain more stretched in the presence of a low amount of CHOL, thus the resulting bilayer thickens. The presence of the hydroxyl group in SM molecules increased the area per lipid and reduced the protrusion of SM headgroups. This was reflected by a thinning of SM/SMh/CHOL membranes compared to the non-hydroxylated bilayers. The presence of groups that can establish hydrogen bonds with water increases the hydration of the bilayer surface if the SM packing is not too tight. At the same time, water molecules bound to the membrane surface were not efficiently oriented in the presence of SMh molecules. The organization of the hydration shell was studied from the dipole moment of water molecules in contact with the membrane surface. The water polarization in the presence of SMh dropped from 0.46 D at CHOL 30% to 0.23 D at CHOL 50% (Table S1, Fig. 1B). High values of water polarization can be observed when a membrane surface is charged, or when it is highly ordered. It is important to notice that polarization changes can affect strongly both membrane electrical potential and orientation of embedded proteins.

The global change in lipid distribution was represented in the mass density profiles of the membranes (Fig. 2). Bilayers with low amounts of CHOL appeared to be thicker and less dense than those with high CHOL levels (Fig. 2A). This tendency was confirmed to a lesser extent in hydroxylated bilayers (Fig. 2B). Bilayers with lower CHOL content had SM molecules in a more elongated conformation and with CHOL closer to the center of the membrane, when compared to CHOL-enriched membranes. Membrane hydroxylation induced a higher mobility of SM headgroups and of CHOL oxygen atoms. The altered distribution of atomic types, and the different orientation of headgroups and lipid chains, had a profound effect on the membrane transversal stress. Fig. 2C–D shows the pressure profile for *Lo* membranes presented above. The pressure profile can be viewed as an indicator of the tendency of a membrane *xy*-plane to expand (positive *p*(*z*) signals) or contract (negative *p*(*z*) signals).

The stress profiles of SM/CHOL membranes were very similar in the headgroup region (Fig. 2C). We observed a reduction of the stress in the hydrophobic (inner) portion of the membrane, which is correlated with a decrease of CHOL content and an increase in membrane fluidity. The incorporation of 2OHOA acts mainly in the inner part of the membrane (Fig. 2C–D). As also evidenced in the RDF and energy analysis, *Lo* membranes with CHOL content smaller than 40% behaved differently than membranes with 40% and 50% CHOL. In more rigid and tightly packed SM:CHOL 6:4 and 5:5 (mol:mol) mixtures, the presence of 2OHOA increased the positive lateral pressure inside the membranes while leaving unchanged the stress in the headgroup region. For the more fluid and less tightly packed SM:CHOL 7:3 and 8:2 (mol:mol) lipid bilayers, 2OHOA reduced the positive pressure in the membrane core as well as the negative stress in the headgroup region. The RDF can provide important information on the water structure around CHOL molecules in membranes. Graphs of Fig. 3 allow giving insights on the water organization around CHOL oxygens. Since the number of oxygens is not constant in all membranes, the values have been normalized. The reduction of CHOL content was accompanied by an increase of the probability to find a water molecule around the CHOL headgroups. Taken together the RDF, thickness and water polarization values, suggest that, at low CHOL ratio, the SM headgroups move toward the water bulk and expose the CHOL oxygens to water molecules. A high degree of water penetration is also indicated by the mass density profiles. The presence of CHOLs from the inner to the surface can trigger conformational change in membrane proteins.

### 3.2. Effect of incorporation of 2OHOA in *Ld* domains

As shown in Fig. 4A, the presence of hydroxylated lipids in POPC and POPC/POPE membranes did not significantly affect the lipid stability. There was a difference with respect to *Lo* membranes, where the energy per lipid did not change compared to the non-hydroxylated ones (see Fig. 1A).

Fig. 4B shows that the thickness of POPC was slightly smaller than most reported values of POPC bilayers due to a higher interdigitation. In contrast to what was observed in the more rigid SM/CHOL

bilayers, the presence of hydroxyl groups induced an increase of the bilayer thickness. Water molecule polarization on a POPC membrane surface was smaller than the one observed in POPC/POPE, as expected in bilayers with more bulky headgroups. Water polarization was also enhanced by the presence of POPCh and POPEh molecules. A POPC:POPCh:POPE:POPEh membrane had a water polarization index similar to that of SM:CHOL 8:2 (mol ratio) membranes. The incorporation of 2OHOA in Ld model membranes induced a similar water reorganization on the membrane surface, as shown in Fig. 4B. Incorporation of 2OHOA did not alter significantly the mass distribution in the membrane; it induced only a slight thickness increase. Fig. 5 permits the comparison of the mass density profiles of POPC/POPE membranes (Fig. 5A) with the corresponding hydroxylated ones (Fig. 5B). The presence of a hydroxylated acyl chain in a membrane increases thickness and chain packing of the bilayers. The stress profile of POPC:POPE in Fig. 5C–D shows a large increase of negative pressure when compared to pure POPC membranes; this is due to the reduced headgroup size of the PE groups that allows a close-fitting surface packing. The negative change in the headgroup region is counterbalanced by a stress increase in the inner portion of the POPC:POPE membrane. The incorporation of 2OHOA has, as expected, only a minor effect on the membranes core. The effect is concentrated in the headgroups regions, within 8 Å, and it is opposite in POPC and POPC:POPE membranes.

The incorporation of 2OHOA in POPC induced a slight increase in the area per lipid (from 58.8 to 59.1 Å<sup>2</sup>), whereas in POPC:POPE membranes we observed a reduction of the mean area per lipid (from 55.6 to 53.6 Å<sup>2</sup>). We have elsewhere observed [31] that the presence of free 2OHOA in POPC membranes was responsible for a more pronounced reduction of the area per lipid (from 58.8 to 55.8 Å<sup>2</sup>), whereas the addition of free 2OHOA to POPC/POPE membranes led to a change similar to that of pre-incorporated 2OHOA into membrane phospholipids (53.5 and 53.6 Å<sup>2</sup> for free 2OHOA and incorporated 2OHOA, respectively).

Taken together with the change in the pressure profile, these data indicate that the incorporation of 2OHOA promotes the emergence of non-lamellar structures in POPC:POPE membranes. It is worth noting that also the presence of free 2OHOA in POPC and POPC:POPE membranes favored the formation of non-lamellar structures, as confirmed by MD [31], and thermal analysis [32].

The RDF of the nitrogen atoms with oxygen atoms of water is shown in Fig. 6. The incorporation of the hydroxyl group in Ld membranes leads to a reduction of water density around the nitrogen atom of POPC (Fig. 6A), POPCh (Fig. 6B), POPE (Fig. 6B), and POPEh (Fig. 6D). Together with the observation of water polarization, these data indicate that the incorporation of 2OHOA makes the membrane surface more compact and less hydrated than normal Ld membranes, though the water molecules appear to be more oriented and polarized.

### 3.3. Raft evolution and dynamics

In order to investigate the effect of the hydroxylation of Ld membranes onto neighbor Lo membranes, we have considered two membrane systems in which a circular raft composed of SM:CHOL (5:5; mol ratio) was immersed in an initially planar, fully hydrated POPC or POPC:POPCh in a 1:1 ratio bilayer. We wanted to analyze whether the incorporation of 2OHOA into POPC could eventually alter raft integrity. The interaction between two membranes of different thickness and fluidity was already considered by Pandit et al. [33] but the incorporation of exogenous fatty acids was not taken into account. Here we focus on three aspects: the area change per lipid, the stability of CHOL molecules in the raft, and the evolution of the raft perimeter. The problem of calculating the correct area per lipid in CHOL:DPPC mixtures has already been addressed elsewhere by Hofsäß et al. [34] and Pandit [33] in two different ways. Hofsäß et al. [34] considered the volumes of the constituent molecules and the simulation cell volume and area. Pandit et al. [33] started by projecting each molecule onto a plane and then generating a Voronoi tessellation. Both methods have some weakness, such as the assumption that the membrane is planar, and that the size of the molecules should be similar. We have employed the same method of Pandit [33] and we obtained the areas per CHOL, SM, and POPC molecule of  $29.5 \pm 0.7$  Å<sup>2</sup>,  $49.8 \pm 1.0$  Å<sup>2</sup>, and  $58.8 \pm 0.9$  Å<sup>2</sup>, respectively. We observed a contraction of areas of POPC closer than 6 Å from the raft from 58.8 to 53.1 Å<sup>2</sup>. This area contraction was accompanied by an increase in the thickness of the POPC bilayer close to the raft. These data suggest that the presence of a Lo region within a Ld region of POPC induces a reorganization of PC molecules to at least 6 Å, and probably an effect can be detected much further. The mobility of the POPC molecules was reduced, and the membrane lateral stress profile changes, rendering the term “Ld region” inappropriate to describe the new physical state.

Fig. 7A shows the lateral view of the POPC:SM:CHOL system after minimization. To evaluate the stability (or the integrity) of the Lo region, we calculated the perimeter of the polygon connecting the

phosphorous atoms of SM molecules at the Lo/Ld border. In the present simulation, in each layer there were 26 atoms and the perimeter evolution was calculated during 50 ns. When the SM:CHOL circular raft is immersed in a POPC bilayer, it remains stable and no deformation can be appreciated (Fig. 7B). The polygon perimeter oscillates between 231 and 236 Å, without losing CHOL molecules. The incorporation of 2OHOA in POPC molecules (Fig. 7C) changes the morphology of the raft and the polygon perimeter oscillates between 240 and 254 Å. The increase of the perimeter is associated to a change in morphology and to the loss of several CHOL molecules. In spite of the lost CHOL and the consequent volume reduction, the perimeter increases, indicating a drastic reorganization of the membrane. At the same time, the reduction in CHOL content is responsible for an increase of fluidity in the inner part of the raft (data not reported).

#### 4. Conclusions

It is well known that modest modifications in fatty acid structure may induce relevant regulatory effects in model lipid membranes [35,36]. 2OHOA is a fatty acid capable of regulating the membrane physical state, the non-lamellar phase propensity and the balance between Lo and Ld membrane domains [37]. The change in the membrane physical state is associated with PKC $\alpha$  translocation to the membrane, followed by overexpression of the CDK inhibitors, p21Cip1 and p27Kip1, and the consequent inactivation of CDKs and E2F-1. At the same time, 2OHOA activates the sphingomyelin synthases, inducing marked increases in the levels of SM (up to over 5 fold) and concomitant decreases in PE [38]. 2OHOA induces also translocation of Ras from the membrane to the cytosol, which causes inactivation of the MAPK and PI3K/Akt pathways [38].

Here we studied Lo and Ld model membranes made of different proportions of SM, CHOL, POPC and POPE, and evaluated how the physical properties of the membranes were modified after incorporation of 2OHOA in the phospholipid structure. We have also simulated a Lo domain of SM/CHOL immersed into a Ld bilayer of POPC, to assess stability of the raft upon incorporation of 2OHOA in the Ld phase.

Confirming a previous observation [24], when the CHOL content in SM/CHOL membranes drops below 40%, the packing is less regular and water can penetrate the membrane surface. The incorporation of 2OHOA into phospholipids changes the lateral stress in the inner part of the membrane, thus affecting the binding of membrane proteins. Moreover, we have seen an increase of CHOL hydration and an increase in bilayer thickness.

The introduction of 2OHOA in POPC and POPC/POPE Ld membranes causes a decrease of lipid stability. The effect is much smaller than the one observed in Lo membranes and goes in the opposite direction, since in Lo systems the presence of hydroxyl SM reduces the energy per molecule. The incorporation of 2OHOA makes the Ld membrane surface more compact and less hydrated than POPC or POPC/POPE membranes, though the water molecules appear to be more oriented and polarized. The stress profile of POPC/POPE shows a large increase of negative pressure when compared to pure POPC membranes; this is due to the reduced headgroup size of the PE groups that allows an efficient surface packing. The negative change in the headgroup region is counterbalanced by a stress increase in the inner portion of the POPC/POPE membrane. POPC is a typical lamellar-prone lipid, whereas POPE, with a smaller headgroup, tends to organize in non-lamellar phases.

The hydroxyl group of 2OHOA increases the propensity of POPC/POPE bilayer to hexagonal or other non-lamellar phases. For Lo/Ld interaction we observed a slight contraction of POPC lipid areas close to the raft. This is accompanied by an increase in thickness of the POPC bilayer. The POPC molecules undergo a reduction in mobility and a change in lateral stress profile that renders the term "Ld region" inappropriate. When a SM/CHOL circular raft is immersed in a POPC bilayer it remains stable and no deformation can be appreciated for the 50 ns of simulation. At the opposite, 50 ns are enough to observe a marked morphology change in a SM/CHOL circular raft when the half of the surrounding POPC lipids are hydroxylated. The raft perimeter increases, in spite of the loss of CHOL molecules and the consequent reduction of the raft volume. In fact, the circular raft undergoes a drastic reorganization. At the same time, the reduction in CHOL content is responsible for an increase of fluidity in the inner part of the raft.

Taken together these data confirm and explain the long term effect of 2OHOA on lipid membranes. We have shown how 2OHOA modulates the physical state of membranes, and we found opposite effects on Lo

and Ld membranes. The incorporation of 2OHOA in membranes can alter raft functionality and, consequently, can alter membrane receptor activity. The change in morphology and the altered lateral pressure profiles are likely to influence the structure and dynamics of membrane proteins. A quantitative

determination of the interaction of hydroxylated membranes with proteins such as sphingomyelin synthases could help clarify the mechanisms of action of 2OHOA and related molecules.

### **Acknowledgements**

MI and DJL are supported by Torres-Quevedo Research Contracts from the Spanish Ministerio de Economía y Competitividad (PTQ-10- 04214 and PTQ-09-02-02113).

### **Abbreviations**

2OHFA: 2-hydroxy fatty acid; 2OHOA: 2-hydroxyoleic acid; CHOL: cholesterol; FFA: free fatty acid; Ld: liquid-disordered; Lo: liquid-ordered; OA: oleic acid; PC: phosphatidylcholine; POPC: 1-palmitoyl-2-oleoyl-sn-glycero-phosphocholine; POPE: 1-palmitoyl-2-oleoyl-sn-glycero-phosphoethanolamine; RMI: R-(+)-2-OHOA; SM: N-oleoyl-D-erythro-sphingosylphosphorylcholine; PUFA: polyunsaturated fatty acid.



## References

- [1] R.C. Pflieger, N.G. Anderson, F. Snyder, Lipid class and fatty acid composition of rat liver plasma membranes isolated by zonal centrifugation, *Biochemistry* 7 (1968) 2826–2833.
- [2] R.D. Klausner, D.K. Bhalla, P. Dragsten, R.L. Hoover, M.J. Karnovsky, Model for capping derived from inhibition of surface receptor capping by free fatty acids, *Proc. Natl. Acad. Sci. U. S. A.* 77 (1980) 437–441.
- [3] R.L. Hoover, K. Fujiwara, R.D. Klausner, D.K. Bhalla, R. Tucker, M.J. Karnovsky, Effects of free fatty acids on the organization of cytoskeletal elements in lymphocytes, *Mol. Cell. Biol.* 1 (1981) 939–948.
- [4] M. Ibarguren, D.J. Lopez, J.A. Encinar, J.M. Gonzalez-Ros, X. Busquets, P.V. Escriba, Partitioning of liquid-ordered/liquid-disordered membrane microdomains induced by the fluidifying effect of 2-hydroxylated fatty acid derivatives, *Biochim. Biophys. Acta* 1828 (2013) 2553–2563.
- [5] M.L. Martin, G. Barceló-Coblijn, R.F. de Almeida, M.A. Noguera-Salva, S. Terés, M. Higuera, G. Liebisch, G. Schmitz, X. Busquets, P.V. Escribá, The role of membrane fatty acid remodeling in the antitumor mechanism of action of 2-hydroxyoleic acid, *Biochim. Biophys. Acta* 1828 (2013) 1405–1413.
- [6] G. Bereziat, Turnover of fatty acids in cellmembranes, *Ann. Nutr. Aliment.* 34 (1980) 241–254.
- [7] H.U. Shetty, Q.R. Smith, K. Washizaki, S.I. Rapoport, A.D. Purdon, Identification of two molecular species of rat brain phosphatidylcholine that rapidly incorporate and turn over arachidonic acid in vivo, *J. Neurochem.* 67 (1996) 1702–1710.
- [8] F. Thies, C. Pillon, P. Moliere, M. Lagarde, J. Lecerf, Preferential incorporation of sn-2 lysoPC DHA over unesterified DHA in the young rat brain, *Am. J. Physiol.* 267 (1994) R1273–1279.
- [9] B.R. Chakravarthy, M.W. Spence, H.W. Cook, Turnover of phospholipid fatty acyl chains in cultured neuroblastoma cells: involvement of deacylation–reacylation and de novo synthesis in plasma membranes, *Biochim. Biophys. Acta* 879 (1986) 264–277.
- [10] P.L. McLennan, T.M. Bridle, M.Y. Abeywardena, J.S. Charnock, Comparative efficacy of n – 3 and n – 6 polyunsaturated fatty acids in modulating ventricular fibrillation threshold in marmoset monkeys, *Am. J. Clin. Nutr.* 58 (1993) 666–669.
- [11] W. Stillwell, L.J. Jenski, F.T. Crump, W. Ehringer, Effect of docosahexaenoic acid on mouse mitochondrial membrane properties, *Lipids* 32 (1997) 497–506.
- [12] Q.S. Tahin, M. Blum, E. Carafoli, The fatty acid composition of subcellular membranes of rat liver, heart, and brain: diet-induced modifications, *Eur. J. Biochem.* 121 (1981) 5–13.
- [13] D.R. Robinson, L.L. Xu, C.T. Knoell, S. Tateno, W. Olesiak, Modification of spleen phospholipid fatty acid composition by dietary fish oil and by n – 3 fatty acid ethyl esters, *J. Lipid Res.* 34 (1993) 1423–1434.
- [14] C.D. Stubbs, A.D. Smith, The modification of mammalian membrane polyunsaturated fatty acid composition in relation to membrane fluidity and function, *Biochim. Biophys. Acta* 779 (1984) 89–137.
- [15] V.T. Armstrong, M.R. Brzustowicz, S.R. Wassall, L.J. Jenski, W. Stillwell, Rapid flip-flop in polyunsaturated (docosahexaenoate) phospholipid membranes, *Arch. Biochem. Biophys.* 414 (2003) 74–82.
- [16] W. Stillwell, S.R. Shaikh, M. Zerouga, R. Siddiqui, S.R. Wassall, Docosahexaenoic acid affects cell signaling by altering lipid rafts, *Reprod. Nutr. Dev.* 45 (2005) 559–579.
- [17] W. Stillwell, S.R. Wassall, Docosahexaenoic acid: membrane properties of a unique fatty acid, *Chem. Phys. Lipids* 126 (2003) 1–27.
- [18] E. Krieger, T. Darden, S.B. Nabuurs, A. Finkelstein, G. Vriend, Making optimal use of empirical energy functions: force-field parameterization in crystal space, *Proteins* 57 (2004) 678–683.
- [19] H.J.C. Berendsen, J.P.M. Postma, W.F. van Gunsteren, A. Di Nola, J.R. Haak, Molecular dynamics with coupling to an external bath, *J. Chem. Phys.* 81 (1984) 3684–3689.

- [20] Y. Duan, C. Wu, S. Chowdhury, M.C. Lee, G. Xiong, W. Zhang, R. Yang, P. Cieplak, R. Luo, T. Lee, A point charge force field for molecular mechanics simulations of proteins based on condensed phase quantum mechanical calculations, *J. Comput. Chem.* 24 (2003) 1999–2012.
- [21] A. Klamt, Conductor-like screening model for real solvents: a new approach to the quantitative calculation of solvation phenomena, *J. Phys. Chem.* 99 (1995) 2224–2235.
- [22] J.J.P. Stewart, *J. Comput. Aided Mol. Des.* 4 (1990) 1–103.
- [23] U. Essmann, L. Perera, M.L. Berkowitz, T. Darden, H. Lee, L.G. Pedersen, A smooth particle mesh Ewald method, *J. Chem. Phys.* 103 (1995) 8577–8593.
- [24] T. Crul, N. Toth, S. Piotto, P. Literati-Nagy, K. Tory, P. Haldimann, B. Kalmar, L. Greensmith, Z. Torok, G. Balogh, Hydroxamic acid derivatives: pleiotropic Hsp co-inducers restoring homeostasis and robustness, *Curr. Pharm. Des.* 19 (2013) 309–346.
- [25] I. Gombos, T. Crul, S. Piotto, B. Gungor, Z. Torok, G. Balogh, M. Peter, J.P. Slotte, F. Campana, A.M. Pilbat, A. Hunya, N. Toth, Z. Literati-Nagy, L. Vigh Jr., A. Glatz, M. Brameshuber, G.J. Schutz, A. Hevener, M.A. Febbraio, I. Horvath, L. Vigh, Membrane-lipid therapy in operation: the HSP co-inducer BGP-15 activates stress signal transduction pathways by remodeling plasma membrane rafts, *PLoS One* 6 (2011) e28818.
- [26] N. Kučerka, S. Tristram-Nagle, J.F. Nagle, Structure of fully hydrated fluid phase lipid bilayers with monounsaturated chains, *J. Membr. Biol.* 208 (2005) 193–202.
- [27] W. Rawicz, K. Olbrich, T. McIntosh, D. Needham, E. Evans, Effect of chain length and unsaturation on elasticity of lipid bilayers, *Biophys. J.* 79 (2000) 328–339.
- [28] R.S. Cantor, The influence of membrane lateral pressures on simple geometric models of protein conformational equilibria, *Chem. Phys. lipids* 101 (1999) 45–56.
- [29] D. Marsh, Lateral pressure in membranes, *Biochim. Biophys. Acta* 1286 (1996) 183–223.
- [30] R.J. Hardy, Formulas for determining local properties in molecular-dynamics simulations: shock waves, *J. Chem. Phys.* 76 (1982) 622–629.
- [31] S. Piotto, S. Concilio, E. Bianchino, P. Iannelli, D.J. López, S. Terés, M. Ibarburen, G. Barceló-Coblijn, M.L. Martin, F. Guardiola-Serrano, M. Alonso-Sande, S.S. Funari, X. Busquets, P.V. Escribá, Differential effect of 2-hydroxyoleic acid enantiomers on protein (sphingomyelin synthase) and lipid (membrane) targets, *Biochim. Biophys. Acta* 1838 (2014) 1628–1637.
- [32] J. Prades, R. Alemany, J.S. Perona, S.S. Funari, O. Vogler, V. Ruiz-Gutiérrez, P.V. Escribá, F. Barceló, Effects of 2-hydroxyoleic acid on the structural properties of biological and model plasma membranes, *Mol. Membr. Biol.* 25 (2008) 46–57.
- [33] S.A. Pandit, S. Vasudevan, S. Chiu, R. JayMashl, E. Jakobsson, H. Scott, Sphingomyelin–cholesterol domains in phospholipid membranes: atomistic simulation, *Biophys. J.* 87 (2004) 1092–1100.
- [34] C. Hofstätter, E. Lindahl, O. Edholm, Molecular dynamics simulations of phospholipid bilayers with cholesterol, *Biophys. J.* 84 (2003) 2192–2206.
- [35] S.S. Funari, F. Barceló, P.V. Escribá, Effects of oleic acid and its congeners, elaidic and stearic acids, on the structural properties of phosphatidylethanolamine membranes, *J. Lipid Res.* 44 (2003) 567–575.
- [36] M. Ibarburen, D.J. López, J.A. Encinar, J.M. González-Ros, X. Busquets, P.V. Escribá, Partitioning of liquid-ordered/liquid-disordered membrane microdomains induced by the fluidifying effect of 2-hydroxylated fatty acid derivatives, *Biochim. Biophys. Acta* 1828 (11) (2013) 2553–2563.
- [37] F. Barceló, J. Prades, S.S. Funari, J. Frau, R. Alemany, P. Escribá, The hypotensive drug 2-hydroxyoleic acid modifies the structural properties of model membranes, *Mol. Membr. Biol.* 21 (2004) 261–268.
- [38] S. Terés, V. Lladó, M. Higuera, G. Barceló-Coblijn, M.L. Martin, M.A. Noguera-Salvà, A. Marcilla-Etxenike, J.M. García-Verdugo, M. Soriano-Navarro, C. Saus, 2-Hydroxyoleate, a nontoxic membrane

binding anticancer drug, induces glioma cell differentiation and autophagy, Proc. Natl. Acad. Sci. 109 (2012) 8489–8494.

**Table 1.** Composition and physical characteristics of the different model membranes studied by means of Molecular Dynamics

Membrane structure	Lipid composition (mol ratio)	Number of lipid molecules	Number of ions and water molecules (Cl <sup>-</sup> :Na <sup>+</sup> :H <sub>2</sub> O)	Simulation box dimensions (Å) (x;y;z)
Lo	SM:CHOL (5:5)	135:137	29:29:10498	74.41;72.96;104
	SM:CHOL (6:4)	146:99	26:26:9264	68.69;70.17;106.25
	SM:CHOL (7:3)	164:72	26:26:9249	69.94;68.36;107.34
	SM:CHOL (8:2)	175:44	26:26:8609	67.31;68.22;106.57
	SM:SMh:CHOL (2.5:2.5:5)	61:61:124	26:26:9382	70.24;70.07;102.74
	SM:SMh:CHOL (3:3:4)	68:68:91	26:26:9287	68.56;69.54;104.28
	SM:SMh:CHOL (3.5:3.5:3)	74:74:64	26:26:8696	67.36;67.73;104.40
	SM:SMh:CHOL (4:4:2)	79:80:41	24:24:7735	64.90;66.33;103.61
Ld	POPC:POPE (10:0)	98:0	24:24:8265	57.18;56.42;120
	POPC:POPE (6:4)	58:40	20:20:7098	56.69;53.79;109.4
	POPC:POPCh (5:5)	49:49	24:24:8265	57.18;56.42;120
	POPC:POPCh:POPE:POPEh (3:3:2:2)	29:29:20:20	20:20:7098	56.69;53.79;109.04
Lo/Ld	POPC:SM:CHOL (7:1.5:1.5)	616:118:118	68:68:23038	99.6;128.35;129.87
	POPC:POPCh:SM:CHOL (3.5:3.5:1.5:1.5)	302:306:113:113	70:70:22324	99.6;128.11;129.73

## Figure legends

**Figure 1.** (A) Histogram showing the potential energy per lipid molecule of Lo membrane models composed of SM:CHOL (filled bars) and SM:SMh:CHOL (gray bars), varying in the CHOL content. (B) Changes in membrane thickness (black lines) and water polarization (grey lines) values of model membranes composed of SM:CHOL (straight lines) and SM:SMh:CHOL (dashed lines) containing different CHOL concentrations.

**Figure 2.** Mass density (A-B) and lateral stress (C-D) profiles of Lo model membranes. Different proportions of non-hydroxylated SM and CHOL were analyzed (straight lines), as well as the incorporation of SMh (dashed lines) in the lipid mixtures. The distribution of water signal to the mass density profile is depicted as a dotted gray line (A-B).

**Figure 3.** Radial distribution function between CHOL oxygen and water oxygen atoms in Lo model membranes containing different proportions of SM:CHOL (A) and SM:SMh:CHOL (B). The difference between the highest and lowest RDF values was included for clarification.

**Figure 4.** (A) Histogram showing the potential energy per lipid molecule of Ld membranes containing non-hydroxylated (filled bars) and hydroxylated (grey bars) phospholipids. Nonhydroxylated lipid mixtures were composed of POPC and POPC:POPE (6:4; mol ratio), while the 2OHOA-containing phospholipid vesicles were formed by POPC:POPCh (5:5; mol ratio) and POPC:POPCh:POPE:POPEh (3:3:2:2; mol ratio). (B) Changes of membrane thickness (black lines) and water polarization (grey lines) values of Ld model membranes as described in (A). Straight lines show lipid mixtures containing non-hydroxylated phospholipids, while hydroxylated lipid mixtures were depicted as dashed lines.

**Figure 5.** Mass density (A-B) and lateral stress (C-D) profiles of Ld model membranes. Different proportions of POPC and POPE were analyzed (panel A and C, straight lines), as well as the incorporation of POPCh and POPEh (panel B and D, dashed lines) in the lipid mixtures. The distribution of water signal to the mass density profile is depicted as a dotted gray line (A-B).

**Figure 6.** Radial distribution function between oxygen atom of water and the nitrogen atom of POPC (A), POPCh (B), POPE (C) and POPEh (D) in Ld model membranes.

**Figure 7.** Circular lipid raft of SM:CHOL (6:4) (Lo) immersed in a POPC bilayer (Ld). CHOL carbons are in yellow, SM carbons in blue, and any other atom is colored according CPK standard. Water and counterions are not shown. (A) Lateral view of the system (B) Top view of a time-sequence changes of the SM:CHOL:POPC system after 0, 25 and 50 ns (C) Time-sequence changes of SM:CHOL lipid raft embedded in a POPC:POPCh (5:5) bilayer system after 0, 25 and 50 ns. The POPCh chain carbon atoms are shown in gray.

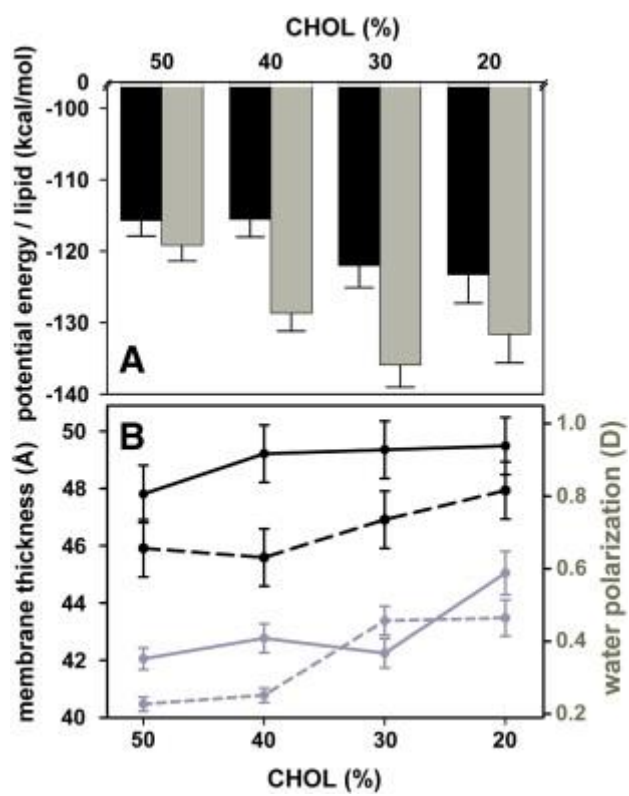


Figure 1

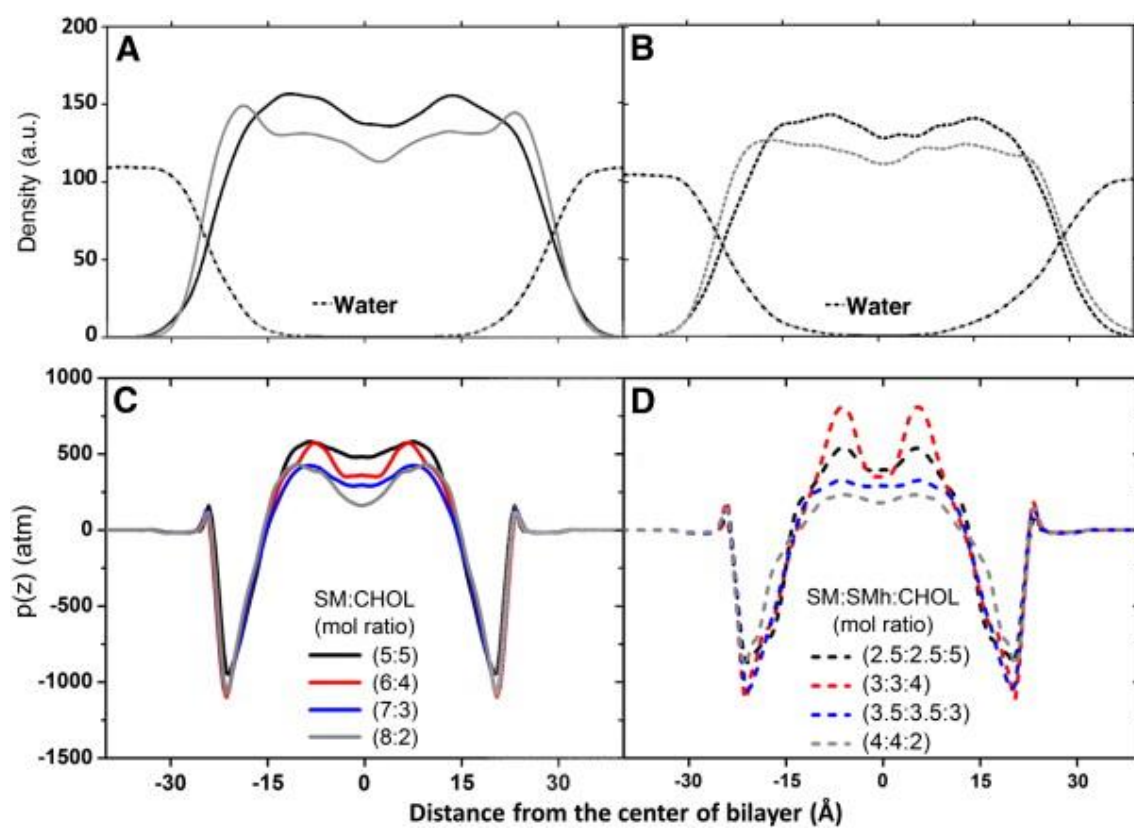


Figure 2

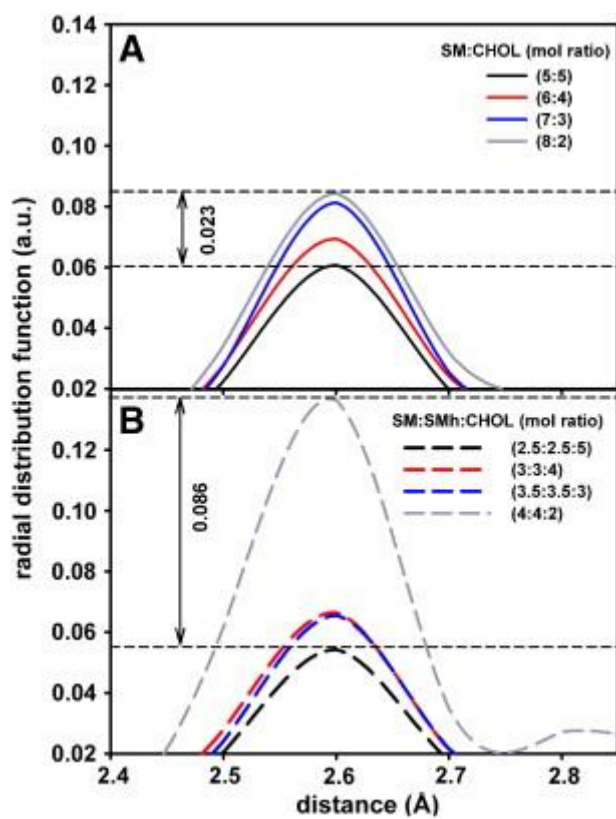


Figure 3



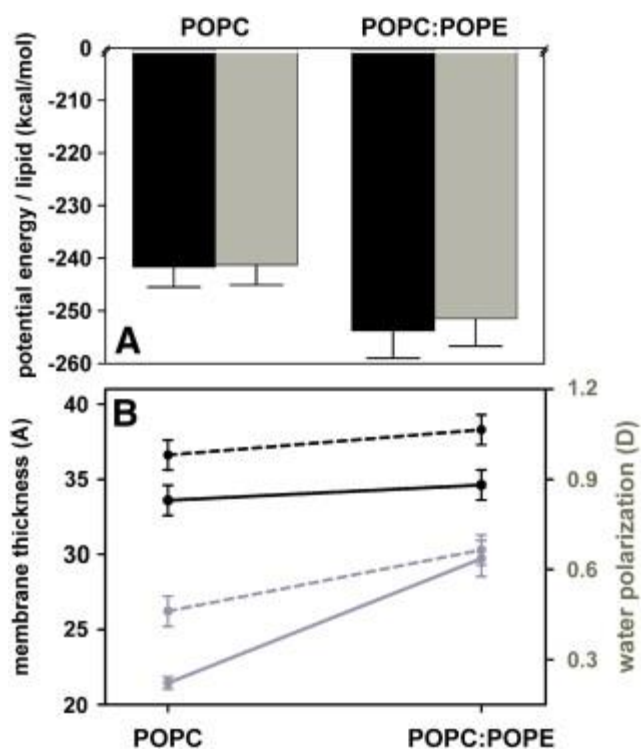


Figure 4

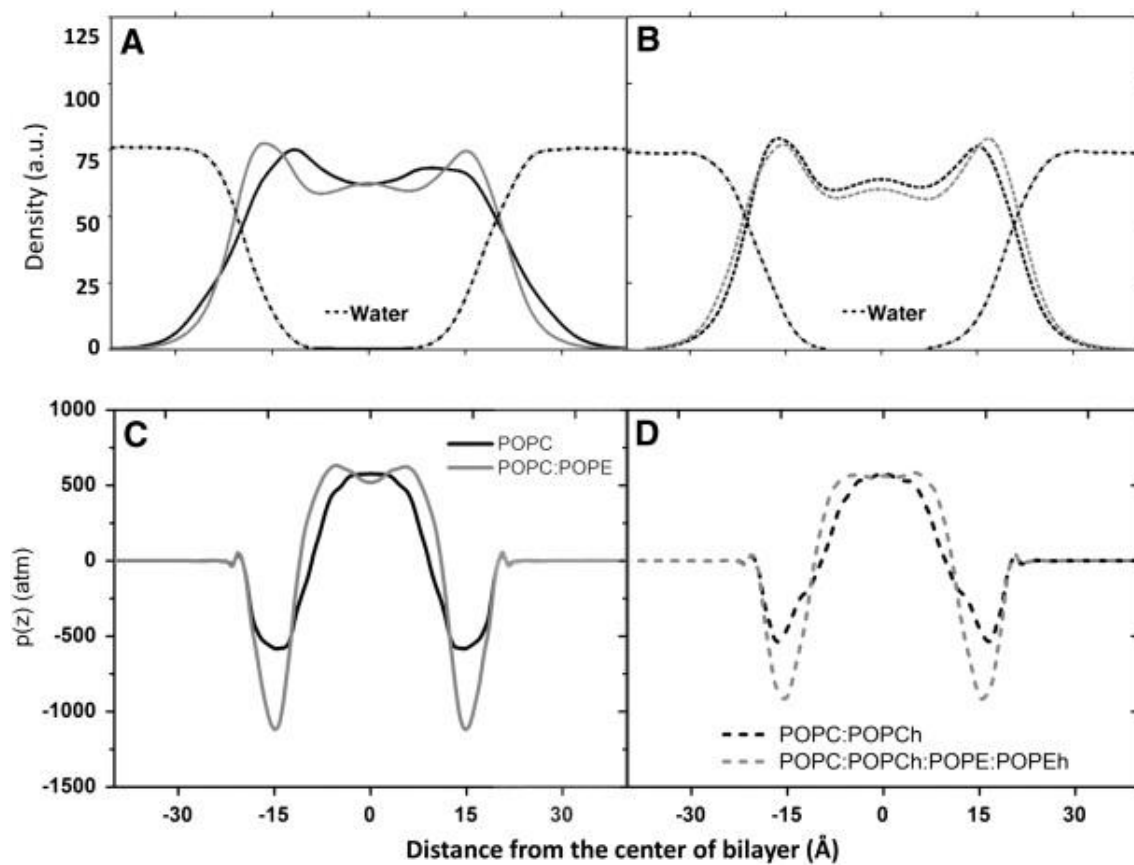


Figure 5

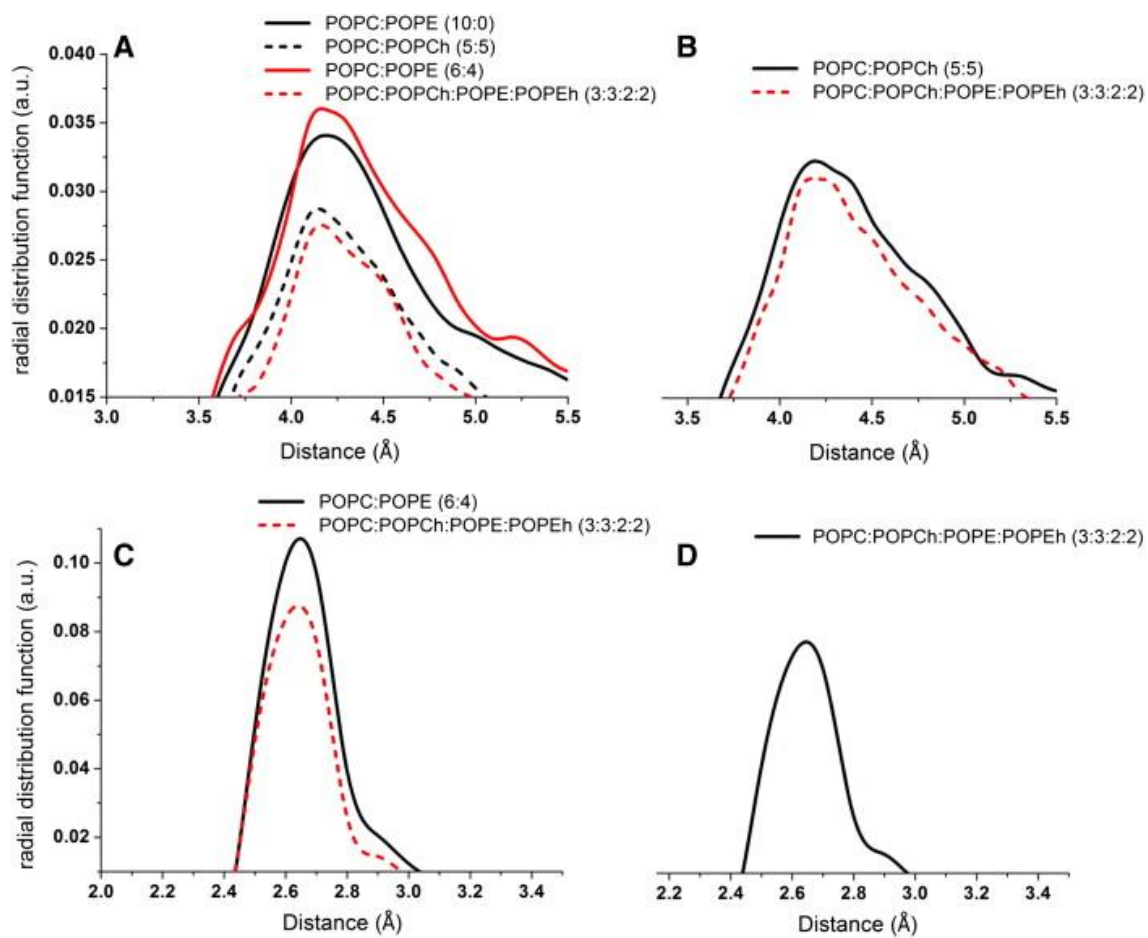


Figure 6

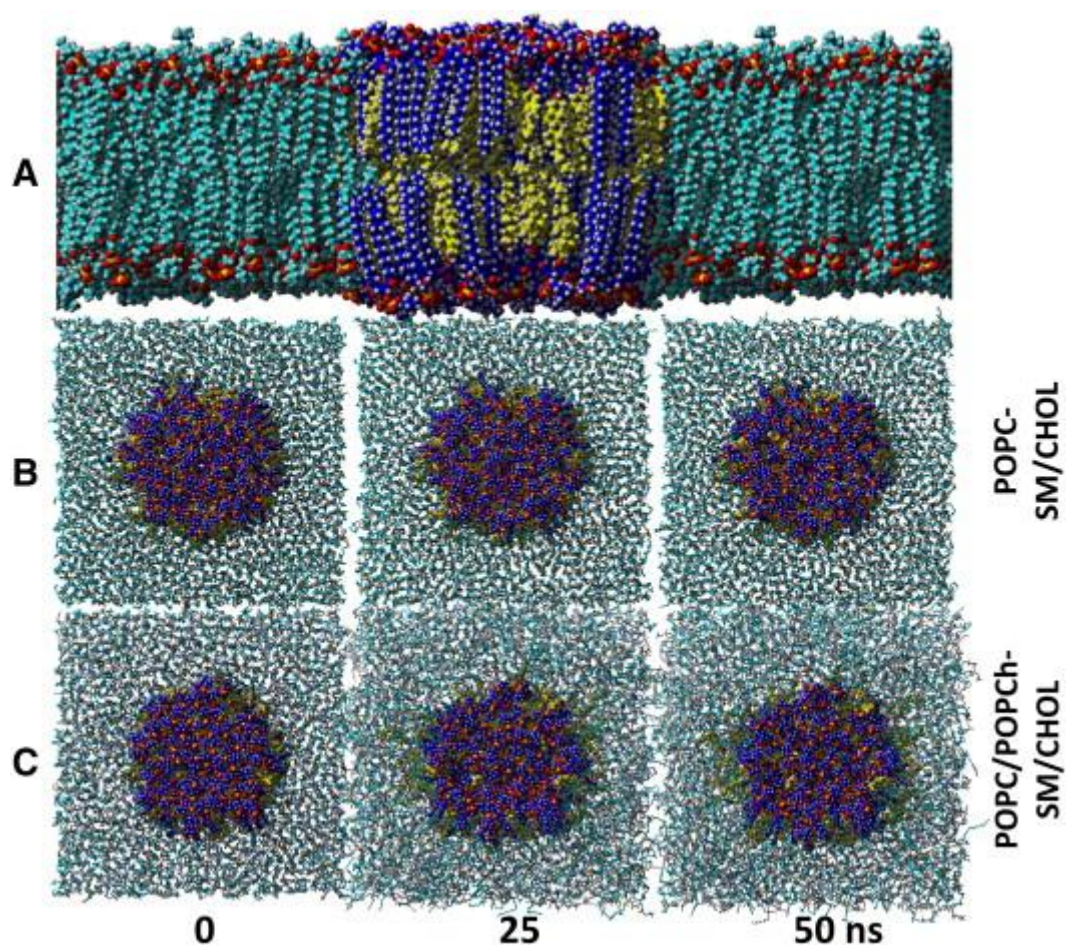
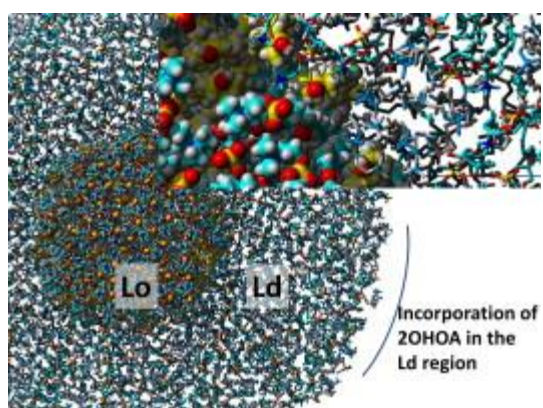


Figure 7



**Graphical abstract**

**Highlights**

- incorporation of 2OHOA renders Ld membrane surface more compact and less hydrated, whereas the opposite effect is observed in Lo domains
- incorporation of 2OHOA in Ld membranes may favor the emergence of non-lamellar structures
- the boundaries between Lo and Ld domains are modified upon incorporation of 2OHOA
- the presence of OH group in POPC induces CHOL leakage from lipid rafts